

Bose-Einstein condensation of trapped polaritons in 2D electron-hole systems in a high magnetic field

Oleg L. Berman¹, Roman Ya. Kezerashvili^{1,2}, and Yurii E. Lozovik³

¹*Physics Department, New York City College of Technology, The City University of New York, Brooklyn, NY 11201, USA*

²*The Graduate School and University Center, The City University of New York, New York, NY 10016, USA*

³*Institute of Spectroscopy, Russian Academy of Sciences, 142190 Troitsk, Moscow Region, Russia*

(Dated: October 8, 2018)

The Bose-Einstein condensation (BEC) of magnetoexcitonic polaritons in two-dimensional (2D) electron-hole system embedded in a semiconductor microcavity in a high magnetic field B is predicted. There are two physical realizations of 2D electron-hole system under consideration: a graphene layer and quantum well (QW). A 2D gas of magnetoexcitonic polaritons is considered in a planar harmonic potential trap. Two possible physical realizations of this trapping potential are assumed: inhomogeneous local stress or harmonic electric field potential applied to excitons and a parabolic shape of the semiconductor cavity causing the trapping of microcavity photons. The effective Hamiltonian of the ideal gas of cavity polaritons in a QW and graphene in a high magnetic field and the BEC temperature as functions of magnetic field are obtained. It is shown that the effective polariton mass M_{eff} increases with magnetic field as $B^{1/2}$. The BEC critical temperature $T_c^{(0)}$ decreases as $B^{-1/4}$ and increases with the spring constant of the parabolic trap. The Rabi splitting related to the creation of a magnetoexciton in a high magnetic field in graphene and QW is obtained. It is shown that Rabi splitting in graphene can be controlled by the external magnetic field since it is proportional to $B^{-1/4}$, while in a QW the Rabi splitting does not depend on the magnetic field when it is strong.

PACS numbers: 71.36.+c, 03.75.Hh, 73.20.Mf, 73.21.Fg

I. INTRODUCTION

In the past decade, Bose coherent effects of 2D excitonic polaritons in a quantum well embedded in a semiconductor microcavity have been the subject of theoretical and experimental studies [1, 2]. To obtain polaritons, two mirrors placed opposite each other form a microcavity, and quantum wells are embedded within the cavity at the antinodes of the confined optical mode. The resonant exciton-photon interaction results in the Rabi splitting of the excitation spectrum. Two polariton branches appear in the spectrum due to the resonant exciton-photon coupling. The lower polariton (LP) branch of the spectrum has a minimum at zero momentum. The effective mass of the lower polariton is extremely small, and lies in the range $10^{-5} - 10^{-4}$ of the free electron mass. These lower polaritons form a 2D weakly interacting Bose gas. The extremely light mass of these bosonic quasiparticles, which corresponds to experimentally achievable excitonic densities, result in a relatively high critical temperature for superfluidity, of 100 K or even higher. The reason for such a high critical temperature is that the 2D thermal de Broglie wavelength is inversely proportional to the mass of the quasiparticle.

While at finite temperatures there is no true BEC in any infinite untrapped 2D system, a true 2D BEC quantum phase transition can be obtained in the presence of a confining potential [3, 4]. Recently, the polaritons in a harmonic potential trap have been studied experimentally in a GaAs/AlAs quantum well embedded in a GaAs/AlGaAs microcavity [5]. In this trap, the exciton energy is shifted using a stress-induced band-gap. In this system, evidence for the BEC of polaritons in a quantum well has been observed [6]. The theory of the BEC and superfluidity of excitonic polaritons in a quantum well without magnetic field in a parabolic trap has been developed in Ref. [7]. The Bose condensation of polaritons is caused by their bosonic character [6, 7, 8].

While the 2D electron system was studied in quantum wells [9] in the past decade, a novel type of 2D electron system was experimentally obtained in graphene, which is a 2D honeycomb lattice of the carbon atoms that form the basic planar structure in graphite [10, 11]. Due to unusual properties of the band structure, electronic properties of graphene became the object of many recent experimental and theoretical studies [10, 11, 12, 13, 14, 15, 16]. Graphene is a gapless semiconductor with massless electrons and holes which have been described as Dirac-fermions [17]. The unique electronic properties in graphene in a magnetic field have been studied recently [18, 19, 20, 21]. The electron-photon interaction in graphene was discussed, for example, in Ref. [22]. The energy spectrum and the wavefunctions of magnetoexcitons, or electron-hole pairs in a magnetic field, in graphene have been calculated in interesting works [23, 24].

The spatially-indirect excitons in coupled quantum wells (CQWs), with and without a magnetic field B have been studied recently experimentally in Refs. [25, 26, 27, 28]. The experimental and theoretical interest in these systems is particularly due to the possibility of the BEC and superfluidity of indirect excitons, which can manifest in the CQW as persistent electrical currents in each well and also through coherent optical properties and Josephson phenomena [29, 30, 31, 32]. Since the exciton binding energies increase with magnetic field, 2D magnetoexcitons survive in a substantially wider temperature range in high magnetic fields [33, 34, 35, 36, 37, 38, 39]. The BEC and superfluidity of spatially-indirect magnetoexcitons with spatially separated electrons and holes have been studied in graphene bilayer [40] and graphene superlattice [41, 42]. The electron-hole pair condensation in the graphene-based bilayers have been studied in [43, 44, 45, 46]. However, the polaritons in graphene in high magnetic field have not yet been considered. The BEC and superfluidity of cavity polaritons in a QW without a trap were considered in [47, 48]. It is interesting to study a 2D system such as polaritons in graphene embedded in a microcavity from the point of view of the existence of the BEC within it.

The purpose of this paper is to point out the existence of the BEC of the magnetoexcitonic polaritons in a QW and a graphene layer embedded in a semiconductor microcavity in a strong magnetic field and to discuss the condition of its realization. Since it was shown that the magnetoexcitons in a QW and graphene layer in a high magnetic field can be described by the same effective Hamiltonian with the different effective mass of a magnetoexciton [41, 42], we expect to obtain the similar expressions for the critical temperature of BEC for cavity polaritons in a QW and graphene with the only difference in the effective mass of a magnetoexciton.

The paper is organized in the following way. In Sec. II the spectrum of an isolated magnetoexciton with the electron and hole in a single graphene layer and QW is derived by applying perturbation theory with respect to the strength of the Coulomb electron-hole attraction. In Sec. III the effective Hamiltonian of microcavity polaritons in graphene and QW in a high magnetic field along with a trapping potential is derived. In Sec. IV the Rabi splitting related to the creation of a magnetoexciton in graphene and QW in a high magnetic field is obtained. The temperature of BEC and the number of polaritons in Bose-Einstein condensate as a function of temperature, magnetic field and spring constant are calculated in Sec. V. Finally, the discussion of the results and conclusions follow in Sec. VI.

II. AN ISOLATED MAGNETOEXCITON IN A SINGLE GRAPHENE LAYER AND QW

When an undoped electron system in graphene in a magnetic field without an external electric field is in the ground state, half of the zeroth Landau level is filled with electrons, all Landau levels above the zeroth one are empty, and all levels below the zeroth one are filled with electrons. We suggest using the gate voltage shown in Fig. 1 to control the chemical potential in graphene by two ways: to shift it above the zeroth level so that it is between the zeroth and first Landau levels (the first case) or to shift the chemical potential below the zeroth level so that it is between the first negative and zeroth Landau levels (the second case). In both cases, all Landau levels below the chemical potential are completely filled and all Landau levels above the chemical potential are completely empty. In the first case, there are allowed transitions between the zeroth and the first Landau levels, while in the second case there are allowed transitions between the first negative and zeroth Landau levels (see the selection rules for optical transitions between the Landau levels in single-layer graphene [49] and the analogous rules for the transitions between Landau levels in a 2D semiconductor [50]). Correspondingly, we consider magnetoexcitons formed in graphene by the electron on the first Landau level and the hole on the zeroth Landau level (the first case) or the electron on the zeroth Landau level and the hole on the Landau level -1 (the second case). Note that by appropriate gate potential we can also use any other neighboring Landau levels n and $n + 1$.

It is obvious that magnetoexcitons formed in graphene are two-dimensional, since graphene is a two-dimensional structure. Below we show that for the relatively high dielectric constant of the microcavity, $\epsilon \gg e^2/(\hbar v_F) \approx 2$ ($v_F = \sqrt{3}at/(2\hbar)$ is the Fermi velocity of electrons in graphene, where $a = 2.566 \text{ \AA}$ is a lattice constant and $t \approx 2.71 \text{ eV}$ is the overlap integral between the nearest carbon atoms [51]) the magnetoexciton energy in graphene can be calculated by applying perturbation theory with respect to the strength of the Coulomb electron-hole attraction analogously as it was done in [33] for 2D quantum wells in a high magnetic field with non-zero electron and hole masses ($m_e \neq 0$ and $m_h \neq 0$). This approach allows us to obtain the spectrum of an isolated magnetoexciton with the electron on the Landau level 1 and the hole on the Landau level 0 in a single graphene layer. The characteristic Coulomb electron-hole attraction for the single graphene layer is $e^2/(er_B)$, where ϵ is the dielectric constant of the environment around graphene, $r_B = \sqrt{\hbar c/(eB)}$ denotes the magnetic length of the magnetoexciton in the magnetic field B , and c is the speed of light. The energy difference between the first and zeroth Landau levels in graphene is $\hbar v_F/r_B$. For graphene, the perturbative approach with respect to the strength of the Coulomb electron-hole attraction is valid when $e^2/(er_B) \ll \hbar v_F/r_B$ [33]. This condition can be fulfilled at all magnetic fields B if the dielectric constant of the surrounding media satisfies the condition $e^2/(\epsilon \hbar v_F) \ll 1$. Therefore, we claim that the energy difference between the first and zeroth Landau levels is always greater than the characteristic Coulomb attraction between the electron

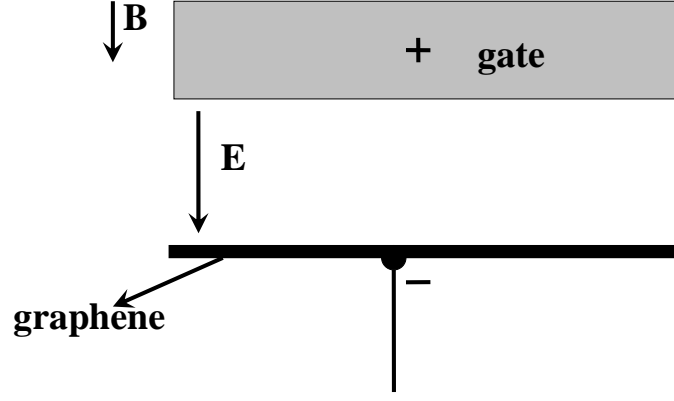


FIG. 1: The graphene sheet in the presence of the applied electric \mathbf{E} and magnetic \mathbf{B} fields.

and the hole in the single graphene layer at any B if $\epsilon \gg e^2/(\hbar v_F) \approx 2$. Thus, applying perturbation theory with respect to weak Coulomb electron-hole attraction in graphene embedded in the GaAs microcavity ($\epsilon = 12.9$) is more accurate than for graphene embedded in the SiO_2 microcavity ($\epsilon = 4.5$). This condition for perturbation theory in graphene is different from the 2D quantum well in GaAs, since in the latter case the energy difference between the neighboring Landau levels is $\hbar\omega_c$, where $\omega_c = eB/(c\mu_{eh})$ is the cyclotron frequency, $\mu_{eh} = m_e m_h / (m_e + m_h)$, and m_e and m_h are the effective masses of the electron and the hole, correspondingly [33]. Therefore, for the quantum well in GaAs, the binding energy of the magnetoexciton is much smaller than the energy difference between two neighboring Landau levels only in the limit of high magnetic field $B \gg e^3 c \mu_{eh}^2 / (\epsilon^2 \hbar^3)$, and perturbation theory with respect to weak electron-hole attraction can be applied only for high magnetic field.

The operator for electron-hole Coulomb attraction is

$$\hat{V}(r) = -\frac{e^2}{\epsilon r}, \quad (1)$$

where $\mathbf{r} = \mathbf{r}_e - \mathbf{r}_h$, and \mathbf{r}_e and \mathbf{r}_h are vectors of an electron and a hole in a 2D plane, respectively.

A conserved quantity for an isolated electron-hole pair in a magnetic field B is the generalized magnetoexciton momentum $\hat{\mathbf{P}}$ [33, 35, 52], which is given by

$$\hat{\mathbf{P}} = -i\hbar\nabla_e - i\hbar\nabla_h + \frac{e}{c}(\mathbf{A}_e - \mathbf{A}_h) - \frac{e}{c}[\mathbf{B} \times (\mathbf{r}_e - \mathbf{r}_h)]. \quad (2)$$

The conservation of $\hat{\mathbf{P}}$ is related to the invariance of the system upon the simultaneous translation of an electron and a hole along with a gauge transformation. In Eq. (2), the cylindrical gauge for the vector potential is used: $\mathbf{A}_{e(h)} = 1/2[\mathbf{B} \times \mathbf{r}_{e(h)}]$.

The eigenfunction ψ_τ of the Hamiltonian of the two-dimensional electron-hole pair in graphene in the perpendicular magnetic field B , which is also the eigenfunction of the generalized momentum $\hat{\mathbf{P}}$, has the form [33, 35, 52]:

$$\psi_{\mathbf{P}}(\mathbf{R}, \mathbf{r}) = \exp \left[i \left(\mathbf{P} + \frac{e}{2c}[\mathbf{B} \times \mathbf{r}] \right) \frac{\mathbf{R}}{\hbar} \right] \tilde{\Phi}(\mathbf{r} - \rho_0), \quad (3)$$

where $\mathbf{R} = (\mathbf{r}_e + \mathbf{r}_h)/2$ and $\rho_0 = c[\mathbf{B} \times \mathbf{P}]/(eB^2)$.

The wave function of the relative coordinate $\tilde{\Phi}(\mathbf{r})$ in Eq. (3) can be expressed in terms of the two-dimensional harmonic oscillator eigenfunctions $\Phi_{n_1, n_2}(\mathbf{r})$. For an electron at the Landau level n_+ and a hole at the level n_- , the four-component wave functions are [23]

$$\tilde{\Phi}_{n_+, n_-}(\mathbf{r}) = \left(\sqrt{2} \right)^{\delta_{n_+, 0} + \delta_{n_-, 0} - 2} \begin{pmatrix} s_+ s_- \Phi_{|n_+|-1, |n_-|-1}(\mathbf{r}) \\ s_+ \Phi_{|n_+|-1, |n_-|}(\mathbf{r}) \\ s_- \Phi_{|n_+|, |n_-|-1}(\mathbf{r}) \\ \Phi_{|n_+|, |n_-|}(\mathbf{r}) \end{pmatrix}, \quad (4)$$

where $s_\pm = \text{sgn}(n_\pm)$.

In a high magnetic field, the magnetoexciton is formed by an electron on the Landau level 1 and a hole on the Landau level 0 with the following four-component wave function:

$$\tilde{\Phi}_{1,0}(\mathbf{r}) = \frac{1}{\sqrt{2}} \begin{pmatrix} 0 \\ \Phi_{0,0}(\mathbf{r}) \\ 0 \\ \Phi_{1,0}(\mathbf{r}) \end{pmatrix}, \quad (5)$$

where $\Phi_{n_1,n_2}(\mathbf{r})$ is the two-dimensional harmonic oscillator eigenfunction given by

$$\Phi_{n_1,n_2}(\mathbf{r}) = (2\pi)^{-1/2} 2^{-|m|/2} \frac{\tilde{n}!}{\sqrt{n_1!n_2!}} \frac{1}{r_B} \text{sgn}(m)^m \frac{r^{|m|}}{r_B^{|m|}} \exp\left[-im\phi - \frac{r^2}{4r_B^2}\right] L_{\tilde{n}}^{|m|}\left(\frac{r^2}{2r_B^2}\right). \quad (6)$$

In Eq. (6), $L_{\tilde{n}}^{|m|}$ denotes Laguerre polynomials, $m = n_1 - n_2$, $\tilde{n} = \min(n_1, n_2)$, and $\text{sgn}(m)^m = 1$ for $m = 0$. Note that we consider a magnetoexciton formed by an electron and a hole located in the same type of valley, e.g., in the point K (or K') of Brillouin zone.

The magnetoexciton energies $E_{n_+,n_-}(P)$ in graphene are functions of the generalized magnetoexciton momentum \mathbf{P} , and in the first-order perturbation, are equal to

$$E_{n_+,n_-}(P) = E_{n_+,n_-}^{(0)} + \mathcal{E}_{n_+,n_-}(P). \quad (7)$$

In Eq. (7), $E_{n_+,n_-}^{(0)}$ is the energy of the electron-hole pair when the electron is at the Landau level n_+ and the hole is at the Landau level n_- , and it is given by [23]

$$E_{n_+,n_-}^{(0)} = \frac{\hbar v_F}{r_B} \sqrt{2} \left[\text{sgn}(n_+) \sqrt{|n_+|} - \text{sgn}(n_-) \sqrt{|n_-|} \right], \quad (8)$$

while

$$\mathcal{E}_{n_+,n_-}(P) = - \left\langle n_+ n_- \mathbf{P} \left| \frac{e^2}{\epsilon r} \right| n_+ n_- \mathbf{P} \right\rangle, \quad (9)$$

where $|n_+ n_- \mathbf{P}\rangle = \psi_{\mathbf{P}}(\mathbf{R}, \mathbf{r})$ is defined by Eq. (3).

We calculate the magnetoexciton energy using the expectation value of the electron-hole Coulomb attraction for an electron on the Landau level 1 and a hole on the Landau level 0. Neglecting the transitions between different Landau levels, the first order perturbation with respect to the weak Coulomb attraction results in the following expression for the energy of the magnetoexciton:

$$E_{1,0}(P) = - \left\langle 1 \ 0 \ \mathbf{P} \left| \frac{e^2}{\epsilon |\mathbf{r}_e - \mathbf{r}_h|} \right| 1 \ 0 \ \mathbf{P} \right\rangle. \quad (10)$$

Denoting the averaging by the 2D harmonic oscillator eigenfunctions $\Phi_{n_1,n_2}(\mathbf{r})$ as $\langle \tilde{n} m \mathbf{P} | \dots | \tilde{n} m \mathbf{P} \rangle_{\Phi}$, where \tilde{n} and m are defined below Eq. (6), we get the energy of a magnetoexciton created by the electron and hole on the lowest Landau level:

$$E_{1,0}(P) = \left\langle 1 \ 0 \ \mathbf{P} \left| \hat{V}(r) \right| 1 \ 0 \ \mathbf{P} \right\rangle = \frac{1}{2} \left(\left\langle 0 \ 0 \ \mathbf{P} \left| \hat{V}(r) \right| 0 \ 0 \ \mathbf{P} \right\rangle_{\Phi} + \left\langle 0 \ 1 \ \mathbf{P} \left| \hat{V}(r) \right| 0 \ 1 \ \mathbf{P} \right\rangle_{\Phi} \right). \quad (11)$$

Following [37], it is easy to show that, for small magnetic momenta $P \ll \hbar/r_B$ for the electron-hole Coulomb attraction (1), each matrix element in Eq. (11) can be expressed in terms of the binding energy and the effective magnetic mass of the magnetoexciton formed by an electron and a hole in the quantum well with the 2D electrons and holes:

$$\langle \tilde{n} m \mathbf{P} | \hat{V}(r) | \tilde{n} m \mathbf{P} \rangle_{\Phi} = -\mathcal{E}_{\tilde{n}m}^{(b)} + \frac{P^2}{2M_{\tilde{n}m}(B)}. \quad (12)$$

$\mathcal{E}_{\tilde{n}m}^{(b)}$ and $M_{\tilde{n}m}(B)$ are the binding energy and the effective magnetic mass of the magnetoexciton, respectively, corresponding to the magnetoexciton in the state with quantum numbers \tilde{n} and m .

Substituting Eq. (12) into Eq. (11), we get the dispersion law of a magnetoexciton for small magnetic momenta

$$E_{1,0}(P) = \frac{1}{2} \left(\mathcal{E}_{00}^{(b)}(B) + \mathcal{E}_{01}^{(b)}(B) \right) + \frac{1}{2} \left(\frac{1}{M_{00}(B)} + \frac{1}{M_{01}(B)} \right) \frac{P^2}{2}. \quad (13)$$

Eq. (13) can be rewritten in the form:

$$E_{1,0}(P) = -\mathcal{E}_B^{(b)} + \frac{P^2}{2m_B}, \quad (14)$$

where the binding energy $\mathcal{E}_B^{(b)}$ and the effective magnetic mass m_B of a magnetoexciton in graphene with the electron on the Landau level 1 and the hole on the Landau level 0 are

$$\begin{aligned} \mathcal{E}_B^{(b)} &= -\frac{1}{2} \left(\mathcal{E}_{00}^{(b)}(B) + \mathcal{E}_{01}^{(b)}(B) \right), \\ \frac{1}{m_B} &= \frac{1}{2} \left(\frac{1}{M_{00}(B)} + \frac{1}{M_{01}(B)} \right). \end{aligned} \quad (15)$$

The constants $\mathcal{E}_{00}^{(b)}(B)$, $\mathcal{E}_{01}^{(b)}(B)$, $M_{00}(B)$, and $M_{01}(B)$ depend on the magnetic field B , and are given in Ref. [37]:

$$\begin{aligned} \mathcal{E}_{00}^{(b)}(B) &= -\mathcal{E}_0, \\ \mathcal{E}_{01}^{(b)}(B) &= -\frac{1}{2}\mathcal{E}_0, \\ M_{00}(B) &= M_0, \\ M_{01}(B) &= -2M_0, \end{aligned} \quad (16)$$

where \mathcal{E}_0 is the magnetoexcitonic energy and M_0 is the effective magnetoexciton mass in a quantum well. These quantities are defined as

$$\begin{aligned} \mathcal{E}_0 &= \sqrt{\frac{\pi}{2}} \frac{e^2}{\epsilon r_B}, \\ M_0 &= \frac{2^{3/2} \epsilon \hbar^2}{\sqrt{\pi} e^2 r_B}. \end{aligned} \quad (17)$$

Substituting Eq. (16) into Eq. (15) gives the binding energy $\mathcal{E}_B^{(b)}$ and the effective magnetic mass m_B of the magnetoexciton in a single graphene layer in a high magnetic field:

$$\mathcal{E}_B^{(b)} = \frac{3}{4}\mathcal{E}_0 = \frac{3}{4}\sqrt{\frac{\pi}{2}} \frac{e^2}{\epsilon r_B}, \quad m_B = 4M_0 = \frac{2^{7/2} \epsilon \hbar^2}{\sqrt{\pi} e^2 r_B}. \quad (18)$$

We can see that the effective magnetic mass of a 2D direct magnetoexciton is 4 times higher in graphene than in a quantum well, while the magnetoexcitonic energy is 3/4 times lower in graphene than in a quantum well at the same ϵ and \mathbf{B} . It is interesting to mention that we obtained the effective magnetic mass of the magnetoexciton in Eq. (18) using the four-component wavefunctions of magnetoexcitons in graphene given by Eqs. (4) and (5). This reflects the specific and different properties of magnetoexcitons and, therefore, magnetopolaritons in graphene compared to the polaritons in a quantum well without a magnetic field [7].

At small magnetic momentum ($P \ll \hbar/r_B$) for measuring energies relative to the binding energy of a magnetoexciton, the dispersion relation $\varepsilon_k(P)$ of a magnetoexciton is quadratic:

$$\varepsilon_k(\mathbf{P}) = \frac{P^2}{2m_{Bk}}, \quad (19)$$

where m_{Bk} is the effective magnetic mass that depends on B and the magnetoexcitonic quantum numbers $k = \{n_+, n_-\}$ for an electron at Landau level n_+ and a hole at level n_- .

It is easy to see that the results for the binding energy and effective magnetic mass of the exciton with the electron on the Landau level 0 and the hole on the Landau level -1 will be exactly the same as for the exciton with the electron on the Landau level 1 and the hole on the Landau level 0.

We have derived above the spectrum of the single magnetoexciton in graphene (14), which is described by the eigenfunction of Dirac equation that has the four-component spinor structure given by Eq. (5). Alternatively, the wave function of the magnetoexciton in a QW has the one-component structure, because this wave function is the eigenfunction of Schrödinger equation. However, Eq. (14) is valid also for a QW, but the binding energy and effective magnetic mass of 2D magnetoexciton formed by the electron and hole in the QW on the zeroth Landau level are given by [33]

$$\mathcal{E}_B^{(b)} = \mathcal{E}_0 = \sqrt{\frac{\pi}{2}} \frac{e^2}{\epsilon r_B}, \quad m_B = M_0 = \frac{2^{3/2} \epsilon \hbar^2}{\sqrt{\pi} e^2 r_B}. \quad (20)$$

Also for a QW the expression for the single magnetoexciton spectrum given by Eq. (19) is valid.

III. THE EFFECTIVE HAMILTONIAN OF TRAPPED MICROCAVITY POLARITONS IN GRAPHENE AND IN A QW IN A HIGH MAGNETIC FIELD

Polaritons are linear superpositions of excitons and photons. In high magnetic fields, when magnetoexcitons may exist, the polaritons become linear superpositions of magnetoexcitons and photons. Let us define the superpositions of magnetoexcitons and photons as magnetopolaritons. It is obvious that magnetopolaritons in graphene are two-dimensional, since graphene is a two-dimensional structure. The effective Hamiltonian of magnetopolaritons in graphene and a QW in the strong magnetic field is given by

$$\hat{H}_{tot} = \hat{H}_{mex} + \hat{H}_{ph} + \hat{H}_{mex-ph} , \quad (21)$$

where \hat{H}_{ph} is a photonic Hamiltonian, and \hat{H}_{mex-ph} is the Hamiltonian of magnetoexciton-photon interaction, and \hat{H}_{mex} is a effective magnetoexcitonic Hamiltonian. Let us analyze each term of the Hamiltonian for magnetopolaritons (21). It was shown in Ref. [41, 42] that 2D magnetoexcitons in graphene and a QW in a high magnetic field can be described by the same effective Hamiltonian \hat{H}_{mex} . The effective Hamiltonian of 2D non-interacting magnetoexcitons in the infinite homogeneous system in a high magnetic field is given by [41, 42]

$$\hat{H}_{mex} = \sum_{\mathbf{P}} \varepsilon_{mex}(P) \hat{b}_{\mathbf{P}}^{\dagger} \hat{b}_{\mathbf{P}} , \quad (22)$$

where $\hat{b}_{\mathbf{P}}^{\dagger}$ and $\hat{b}_{\mathbf{P}}$ are magnetoexcitonic creation and annihilation operators obeying the Bose commutation relations. For Hamiltonian (22), the energy dispersion of a single magnetoexciton in a graphene layer is given by

$$\varepsilon_{mex}(P) = E_{band} - \mathcal{E}_B^{(b)} + \varepsilon_0(P) . \quad (23)$$

$E_{band} = E_{1,0}^{(0)} = \sqrt{2}\hbar v_F/r_B$ is the band gap energy, which is the difference between the Landau levels 1 and 0 in graphene defined by Eq. (8). $\mathcal{E}_B^{(b)}$ is the binding energy of a 2D magnetoexciton with the electron in the Landau level 1 and the hole on the Landau level 0 in a single graphene layer, and $\varepsilon_0(P) = P^2/(2m_B)$, where m_B is the effective magnetic mass of a 2D magnetoexciton with the electron on the Landau level 1 and hole on the Landau level 0 in a single graphene layer given by Eq. (19).

It can be shown that the interaction between two direct 2D magnetoexcitons in graphene with the electron on the Landau level 1 and the hole on the Landau level 0 can be neglected in a strong magnetic field, in analogy to what is described in Ref. [33] for 2D magnetoexcitons in a quantum well. The dipole moment of each exciton in a magnetic field is $\mathbf{d}_{1,2} = e\rho_0 = r_B^2 [\mathbf{B} \times \mathbf{P}_{1,2}]/B$ [33], where \mathbf{P}_1 and \mathbf{P}_2 are the magnetic momenta of each exciton and $P_1, P_2 \ll 1/r_B$. The magnetoexcitons are located at a distance $R \gg r_B$ from each other. The corresponding contribution to the energy of their dipole-dipole interaction is $\sim \mathcal{E}_B^{(b)} (r_B/R)^3 P_1 P_2 r_B^2 / \epsilon \sim (r_B/R)^3 P_1 P_2 / (\epsilon M_0) \ll e^2 r_B^2 / (\epsilon R^3)$. Inputting the radius of the magnetoexciton in graphene $r_{0,1} \sim r_B$ [40], we obtain that the van der Waals attraction of the exciton at zero momenta is proportional to $\sim (r_{0,1}/R)^6 \sim (r_B/R)^6$. Therefore, in the limit of a strong magnetic field for a dilute system $r_B \ll R$, both the dipole-dipole interaction and the van der Waals attraction vanish, and the 2D magnetoexcitons in graphene form an ideal Bose gas analogously to the 2D magnetoexcitons in a quantum well given in Ref. [33]. Thus, the Hamiltonian (21) does not include the term corresponding to the interaction between two direct magnetoexcitons in a single graphene layer. So in high magnetic field there is the BEC of the ideal magnetoexcitonic gas in graphene.

Let us analyze the other two terms in the Hamiltonian (21). The Hamiltonian of non-interacting photons in a semiconductor microcavity is given by [53]:

$$\hat{H}_{ph} = \sum_{\mathbf{P}} \varepsilon_{ph}(P) \hat{a}_{\mathbf{P}}^{\dagger} \hat{a}_{\mathbf{P}} , \quad (24)$$

where $\hat{a}_{\mathbf{P}}^{\dagger}$ and $\hat{a}_{\mathbf{P}}$ are photonic creation and annihilation Bose operators. The cavity photon spectrum is given by

$$\varepsilon_{ph}(P) = (c/n) \sqrt{P^2 + \hbar^2 \pi^2 L_C^{-2}} . \quad (25)$$

In Eq. (25), L_C is the length of the cavity, $n = \sqrt{\epsilon_C}$ is the effective refractive index and ϵ_C is the dielectric constant of the cavity. We assume that the length of the microcavity has the following form:

$$L_C(B) = \frac{\hbar \pi c}{n (E_{band} - \mathcal{E}_B^{(b)})} , \quad (26)$$

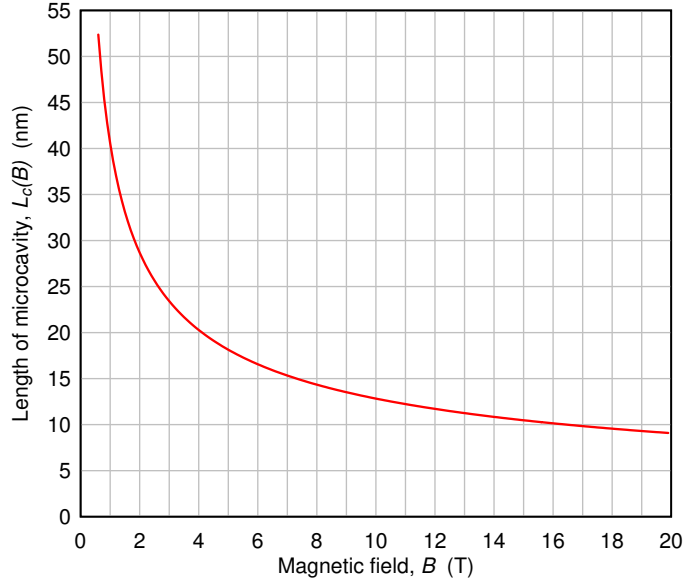


FIG. 2: The length of the microcavity of GaAs ($\epsilon_C = 12.9$), corresponding to magnetoexciton-photon resonance, as a function of the magnetic field B .

corresponding to the resonance of the photonic and magnetoexcitonic branches at $P = 0$ (i.e. $\epsilon_{mex}(0) = \epsilon_{ph}(0)$). The length of the microcavity, corresponding to a magnetoexciton-photon resonance, decreases with the increment of the magnetic field as $B^{-1/2}$. The dependence of the length of the microcavity corresponding to the magnetoexciton-photon resonance on the magnetic field is shown in Fig. 2. The resonance between magnetoexcitons and cavity photonic modes can be achieved either by controlling the spectrum of magnetoexcitons $\epsilon_{ex}(P)$ by changing magnetic field B or by choosing the appropriate length of the microcavity L_C . Let us mention that, while in the presence of a high magnetic field, the length of the microcavity corresponding to the magnetoexciton-photon resonance depends on the magnetic field as it is shown in Fig. 2. This effect does not take place in the system without a magnetic field [7].

The Hamiltonian of the harmonic magnetoexciton-photon coupling has the form [54]:

$$\hat{H}_{mex-ph} = \hbar\Omega_R \sum_{\mathbf{P}} \hat{a}_{\mathbf{P}}^\dagger \hat{b}_{\mathbf{P}} + h.c., \quad (27)$$

where the magnetoexciton-photon coupling energy represented by the Rabi constant $\hbar\Omega_R$ is obtained in Sec. IV. Let us mention that Ω_R is obtained for a QW from the standard procedure describing the electron-photon interaction in the Hamiltonian by the $\mathbf{P} \cdot \mathbf{A}$ term, while in a single graphene layer Ω_R is obtained from the electron-photon interaction based on the Dirac Hamiltonian for the electron in graphene.

The excitonic and photonic operators are defined as [54]

$$\hat{b}_{\mathbf{P}} = X_P \hat{p}_{\mathbf{P}} - C_P \hat{u}_{\mathbf{P}}, \quad \hat{a}_{\mathbf{P}} = C_P \hat{p}_{\mathbf{P}} + X_P \hat{u}_{\mathbf{P}}, \quad (28)$$

where $\hat{p}_{\mathbf{P}}$ and $\hat{u}_{\mathbf{P}}$ are lower and upper magnetopolariton Bose operators, respectively. X_P and C_P are given by

$$X_P = \frac{1}{\sqrt{1 + \left(\frac{\hbar\Omega_R}{\epsilon_{LP}(P) - \epsilon_{ph}(P)}\right)^2}}, \quad C_P = -\frac{1}{\sqrt{1 + \left(\frac{\epsilon_{LP}(P) - \epsilon_{ph}(P)}{\hbar\Omega_R}\right)^2}}, \quad (29)$$

and the energy spectra of the lower/upper magnetopolaritons are

$$\begin{aligned} \epsilon_{LP/UP}(P) &= \frac{\epsilon_{ph}(P) + \epsilon_{mex}(P)}{2} \\ &\mp \frac{1}{2} \sqrt{(\epsilon_{ph}(P) - \epsilon_{mex}(P))^2 + 4|\hbar\Omega_R|^2}. \end{aligned} \quad (30)$$

Eq. (30) implies a splitting of $2\hbar\Omega_R$ between the upper and lower states of polaritons at $P = 0$, which is known as the Rabi splitting. Let us also mention that $|X_P|^2$ and $|C_P|^2 = 1 - |X_P|^2$ represent the magnetoexciton and cavity photon fractions in the lower magnetopolariton.

Substituting Eq. (28) into Eqs. (22), (24) and (27), we conclude that the total Hamiltonian \hat{H}_{tot} (21) can be diagonalized by applying unitary transformations (28) and has the form:

$$\hat{H}_{tot} = \sum_{\mathbf{P}} \varepsilon_{LP}(P) \hat{p}_{\mathbf{P}}^\dagger \hat{p}_{\mathbf{P}} + \sum_{\mathbf{P}} \varepsilon_{UP}(P) \hat{u}_{\mathbf{P}}^\dagger \hat{u}_{\mathbf{P}}, \quad (31)$$

where $\hat{p}_{\mathbf{P}}^\dagger$, $\hat{p}_{\mathbf{P}}$, $\hat{u}_{\mathbf{P}}^\dagger$, $\hat{u}_{\mathbf{P}}$ are the Bose creation and annihilation operators for the lower and upper magnetopolaritons, respectively.

Eq. (31) is the Hamiltonian of magnetopolaritons in a single graphene layer in a high magnetic field. Our particular interest is the lower energy magnetopolaritons which produce the BEC. The lower polaritons have the lowest energy within a single graphene layer. Therefore, from Eq. (31) we can obtain

$$\hat{H}_{tot} = \sum_{\mathbf{P}} \varepsilon_{LP}(P) \hat{p}_{\mathbf{P}}^\dagger \hat{p}_{\mathbf{P}}. \quad (32)$$

Similarly to the case of Bose atoms in a trap [55, 56] in the case of a slowly varying external potential, we can make the quasiclassical approximation, assuming that the effective magnetoexciton mass does not depend on a characteristic size l of the trap and it is a constant within the trap. This quasiclassical approximation is valid if $P \gg \hbar/l$. The harmonic trap is formed by the two-dimensional planar potential in the plane of graphene. The potential trap can be produced in two different ways. In case 1, the potential trap can be produced by applying an external inhomogeneous electric field or inhomogeneous local stress. The spatial dependence of the external field potential $V(r)$ is caused by shifting of magnetoexciton energy by applying an external inhomogeneous electric field or inhomogeneous local stress. The photonic states in the cavity are assumed to be unaffected by this electric field or stress. In this case the band energy E_{band} is replaced by $E_{band}(r) = E_{band}(0) + V(r)$. Near the minimum of the magnetoexciton energy, $V(r)$ can be approximated by the planar harmonic potential $\gamma r^2/2$, where γ is the spring constant. Note that a high magnetic field does not change the trapping potential in the effective Hamiltonian [50, 57]. In case 2, the trapping of magnetopolaritons is caused by the inhomogeneous shape of the cavity when the length of the cavity is given by

$$L_C(r) = \frac{\hbar\pi c}{n \left(E_{band} - \mathcal{E}_B^{(b)} + \gamma r^2/2 \right)}, \quad (33)$$

where r is the distance between the photon and the center of the trap. In case 2, the γ in Eq. (33) is the curvature characterizing the shape of the cavity. In case 1, for the slowly changing confining potential $V(r) = \gamma r^2/2$, the magnetoexciton spectrum is given in the effective mass approximation as

$$\varepsilon_{mex}^{(0)}(P) = \varepsilon_{mex}(P) + V(r) = (c/n)\hbar\pi L_C^{-1} + \frac{\gamma}{2}r^2 + \frac{P^2}{2m_B}, \quad (34)$$

where r is now the distance between the center of mass of the magnetoexciton and the center of the trap. The Hamiltonian for photons in this case is given by Eq. (24), the spectrum of photons is shown by Eq. (25) and the length of the microcavity is given by Eq. (26).

In case 2, for the slowly changing shape of the length of cavity given by Eq. (33), the photonic spectrum is given in the effective mass approximation as

$$\varepsilon_{ph}^{(0)}(P) = (c/n) \sqrt{P^2 + \frac{n^2}{c^2} \left(E_{band} - \mathcal{E}_B^{(b)} + \frac{\gamma r^2}{2} \right)}. \quad (35)$$

This quasiclassical approximation is valid if $P \gg \hbar/l$, where $l = (\hbar/(m_B\omega_0))^{1/2}$ is the size of the magnetoexciton cloud in an ideal magnetoexciton gas and $\omega_0 = \sqrt{\gamma/m_B}$. The Hamiltonian and spectrum of magnetoexcitons in this case are given by Eq. (22) and (23), correspondingly.

The total Hamiltonian \hat{H}_{tot} can be diagonalized by applying unitary transformations. At small momenta $\alpha \equiv 1/2(m_B^{-1} + (c/n)L_C/\hbar\pi)P^2/|\hbar\Omega_R| \ll 1$ ($L_C = \hbar\pi c/n \left(E_{band} - \mathcal{E}_B^{(b)} \right)^{-1}$) and weak confinement $\beta \equiv \gamma r^2/|\hbar\Omega_R| \ll 1$, the single-particle lower magnetopolariton spectrum obtained through the substitution of Eq. (34) into Eq. (30), in linear order with respect to the small parameters α and β , is

$$\varepsilon_0(P) \approx \frac{c}{n} \hbar\pi L_C^{-1} - |\hbar\Omega_R| + \frac{\gamma}{4}r^2 + \frac{1}{4} \left(m_B^{-1} + \frac{cL_C(B)}{n\hbar\pi} \right) P^2. \quad (36)$$

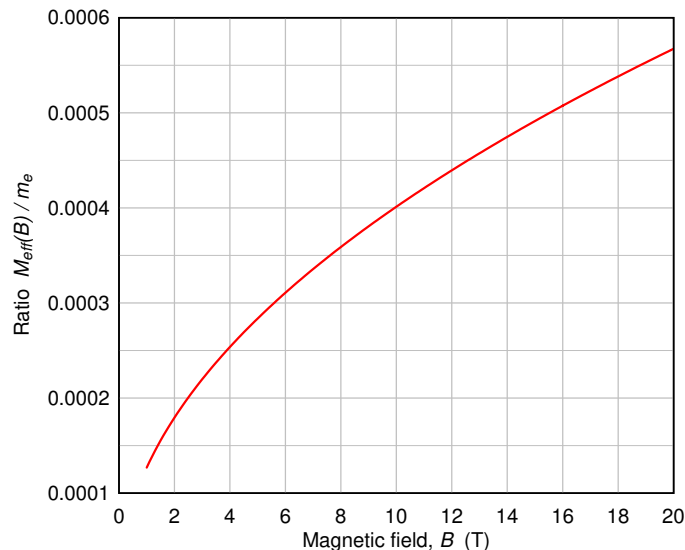


FIG. 3: The ratio of the effective magnetopolariton mass $M_{\text{eff}}(B)$ to the mass of a free electron m_e as a function of magnetic field B .

Let us emphasize that the spectrum of non-interacting magnetopolaritons $\varepsilon_0(P)$ at small momenta and weak confinement is given by Eq. (36) for both physical realizations of confinement: case 1 and case 2. By substituting Eq. (34) into Eq. (29), we obtain $X_{\mathbf{P}} \approx 1/\sqrt{2}$. The condition for the validity of the quasiclassical approach in Eq. (22), $Pl \gg \hbar$, is also applied here.

If we measure the energy relative to the $P = 0$ lower magnetopolariton energy $(c/n)\hbar\pi L_C^{-1} - |\hbar\Omega_R|$, we obtain the resulting effective Hamiltonian for trapped magnetopolaritons in graphene in a magnetic field. At small momenta $\alpha \ll 1$ ($L_C = \hbar\pi c/n (E_{\text{band}} - \mathcal{E}_B^{(b)})^{-1}$) and weak confinement $\beta \ll 1$, this effective Hamiltonian is

$$\hat{H}_{\text{eff}} = \sum_{\mathbf{P}} \left(\frac{P^2}{2M_{\text{eff}}(B)} + \frac{1}{2}V(r) \right) \hat{p}_{\mathbf{P}}^\dagger \hat{p}_{\mathbf{P}}, \quad (37)$$

where the sum over \mathbf{P} is carried out only over $P \gg \hbar/l$ (only in this case the quasiclassical approach used in Eq. (34) is valid), and the effective magnetic mass of a magnetopolariton is given by

$$M_{\text{eff}}(B) = 2 \left(m_B^{-1} + \frac{cL_C(B)}{n\hbar\pi} \right)^{-1}. \quad (38)$$

According to Eq. (38), the effective magnetopolariton mass M_{eff} increases with the increment of the magnetic field as $B^{1/2}$, as shown in Fig. 3. Let us emphasize that the resulting effective Hamiltonian for magnetopolaritons in graphene in a magnetic field for the parabolic trap is given by Eq. (37) for both physical realizations of confinement represented by case 1 and case 2. The effective magnetic mass of the magnetopolariton in a QW is approximately the same as in graphene, since the contribution to $M_{\text{eff}}(B)$ from the second term in the r.h.s. of Eq. (38) is much higher than from the first term. So the effective mass of the magnetopolariton in a QW can also be presented by Fig. 3.

Let us mention that the effective Hamiltonian of magnetopolaritons in a QW in microcavity is also given by Eq. (37) with the effective magnetic mass of magnetoexciton with the electron and hole on the zeroth Landau level provided by Eq. (20).

IV. THE RABI SPLITTING CONSTANT IN GRAPHENE AND A QW IN HIGH MAGNETIC FIELD

Neglecting anharmonic terms for the magnetoexciton-photon coupling, the Rabi splitting constant Ω_R can be estimated quasiclassically as

$$|\hbar\Omega_R| = \left| \left\langle f \left| \hat{H}_{\text{int}} \right| i \right\rangle \right|, \quad (39)$$

where \hat{H}_{int} is the Hamiltonian of the electron-photon interaction. For graphene this interaction is determined by Dirac electron Hamiltonian as

$$\hat{H}_{int} = -\frac{v_F e}{c} \vec{\sigma} \cdot \vec{A}_{ph0} = \frac{v_F e}{i\omega} \vec{\sigma} \cdot \vec{E}_{ph0} , \quad (40)$$

where $\vec{\sigma} = (\hat{\sigma}_x, \hat{\sigma}_y)$, $\hat{\sigma}_x$ and $\hat{\sigma}_y$ are Pauli matrices, \vec{A}_{ph0} is the vector potential corresponding to a single cavity photon, and $E_{ph0} = (8\pi\hbar\omega/(\epsilon W))^{1/2}$ is the magnitude of electric field corresponding to a single cavity photon of the frequency ω in the volume of microcavity W , while for the QW this interaction is

$$\hat{H}_{int} = \vec{d}_{12} \cdot \vec{E}_{ph0} , \quad (41)$$

where

$$\vec{d}_{12} = e \sum_i \mathbf{r}_i \quad (42)$$

is the dipole momentum of transition and the sum is taken over the coordinate vectors related to the positions of all the electrons in the system.

In Eq. (39) the initial $|i\rangle$ and final $|f\rangle$ electron states are different for graphene and a quantum well. For the case of graphene these electron states are defined as

$$\begin{aligned} |i\rangle &= \prod_k \hat{c}_{0,k}^\dagger |0\rangle_0 |0\rangle_1 , \\ |f\rangle &= \hat{b}_{1,0}^\dagger |i\rangle . \end{aligned} \quad (43)$$

In Eq. (43), $\hat{c}_{n,k}^\dagger$ is the Fermi creation operator of the electron with the y component of the wavevector k on the Landau level n , $|0\rangle_n$ denotes the wavefunction of the vacuum on the Landau level n , $\prod_k \hat{c}_{0,k}^\dagger |0\rangle_0$ corresponds to the completely filled zeroth Landau level, $\hat{b}_{n,n'}^\dagger$ is the Bose creation operator of the magnetoexciton with the electron on the Landau level n and the hole on the Landau level n' . We consider magnetoexcitons with magnetic momenta equal to zero, for which the Bose condensate in the system of non-interacting particles is the exact solution of the problem [33]. Following Ref. [33] $\hat{b}_{n,n'}^\dagger$ for this case is defined as

$$\hat{b}_{n,n'}^\dagger = \frac{1}{\sqrt{N_d}} \sum_k \hat{h}_{n',k}^\dagger \hat{c}_{n,-k}^\dagger , \quad (44)$$

where $\hat{h}_{n',k}^\dagger$ is the Fermi creation operator of the hole with the y component of the wavevector k on the Landau level n' , $N_d = S/(2\pi r_B^2)$ is the macroscopic degeneracy of Landau levels, and S is the area of the system.

Let us use the Landau gauge for the wavefunction of the single electron $\psi_{n,k}(x, y)$ with the y component of the wavevector k on the Landau level n . In the Landau gauge with the vector potential $\mathbf{A} = (0, Bx, 0)$, the two-component eigenfunction $\psi_{n,k}(\mathbf{r})$ is given by [58]

$$\psi_{n,k}(x, y) = \frac{C_n}{\sqrt{L_y}} \exp(iky) \begin{pmatrix} s(n) i^{n-1} \Phi_{n-1}(x - r_B^2 k) \\ i^n \Phi_n(x - r_B^2 k) \end{pmatrix} , \quad (45)$$

where $s(n)$ defined by

$$s(n) = \begin{cases} 0 & (n = 0) , \\ \pm 1 & (n > 0) . \end{cases} \quad (46)$$

L_y are normalization lengths in the y direction,

$$C_n = \begin{cases} 1 & (n = 0) , \\ 1/\sqrt{2} & (n > 0) , \end{cases} \quad (47)$$

and

$$\Phi_n(x) = (2^n n! \sqrt{\pi} r_B)^{-1/2} \exp \left[-\frac{1}{2} \left(\frac{x}{r_B} \right)^2 \right] H_n \left(\frac{x}{r_B} \right) , \quad (48)$$

where $H_n(x)$ is the Hermite polynomial. The corresponding eigenenergies depend on the quantum number n only and are given by

$$\varepsilon_n = \frac{\hbar v_F}{r_B} \sqrt{2n} . \quad (49)$$

Substituting Eqs. (44) and (45) into (43) and using the electron-photon interaction \hat{H}_{int} (40), we finally obtain from Eq. (39):

$$|\hbar\Omega_R| = \left| \frac{ev_F}{i\omega} \int dx \int dy x \left[\psi_{1,k}^*(x, y) \vec{\sigma} \cdot \vec{E}_{ph0} \psi_{0,k}(x, y) \right] \right| = \frac{ev_F |E_{ph0}|}{\sqrt{2}\omega} . \quad (50)$$

In Eq. (50) the energy of photon absorbed at the creation of the magnetoexciton (at $\mathcal{E}_B^{(b)} \ll \varepsilon_1 - \varepsilon_0$) is given by

$$\hbar\omega = \varepsilon_1 - \varepsilon_0 = \sqrt{2} \frac{\hbar v_F}{r_B} . \quad (51)$$

Substituting the photon energy from Eq. (51) into Eq. (50), we obtain the Rabi splitting corresponding to the creation of a magnetoexciton with the electron on the Landau level 1 and the hole on the Landau level 0 in graphene:

$$\hbar\Omega_R = 2e \left(\frac{\pi \hbar v_F r_B}{\sqrt{2} \epsilon W} \right)^{1/2} . \quad (52)$$

As follows from Eq. (52), the Rabi splitting in graphene is related to the creation of the magnetoexciton, which decreases when the magnetic field increases and is proportional to $B^{-1/4}$. Therefore, the Rabi splitting in graphene can be controlled by the external magnetic field. Note that in a semiconductor quantum well contrary to graphene the Rabi splitting does not depend on the magnetic field.

Substituting Eq. (41) and the initial $|i\rangle$ and final $|f\rangle$ electron states from Ref. [33] into (39) after the integration we obtain the Rabi splitting constant Ω_R for a quantum well

$$\hbar\Omega_R = d_{12} E_{ph0} , \quad (53)$$

where d_{12} is the matrix term of a magnetoexciton generation transition in a QW represented as

$$d_{12} = e \left\langle f \left| \sum_i \mathbf{r}_i \right| i \right\rangle . \quad (54)$$

The similar calculations for the transition dipole moment and the photon energy corresponding to the formation of magnetoexciton with the electron and hole on zeroth Landau level in the QW gives:

$$\begin{aligned} d_{12} &= \frac{er_B}{2\sqrt{2}} , \\ \hbar\omega &= \varepsilon_1 - \varepsilon_0 = \hbar\omega_c = \frac{\hbar e B}{c\mu_{eh}} . \end{aligned} \quad (55)$$

Substituting the transition dipole moment and the photon energy given by Eq. (55) into Eq. (39), we obtain the Rabi splitting for QW:

$$\hbar\Omega_R = 2e\hbar \left(\frac{\pi}{\epsilon\mu_{eh} W} \right)^{1/2} . \quad (56)$$

Thus, as it follows from Eq. (56), the Rabi splitting in a QW does not depend on the magnetic field in the limit of high magnetic field. Therefore, only in graphene can the Rabi splitting be controlled by the external magnetic field in the limit of high magnetic field.

It is easy to show that the Rabi splitting related to the creation of the magnetoexciton, the electron on the Landau level 0 and the hole on the Landau level -1 will be exactly the same as for the magnetoexciton with the electron on the Landau level 1 and the hole on the Landau level 0. Let us mention that dipole optical transitions from the Landau level -1 to the Landau level 0, as well as from the Landau level 0 to the Landau level 1, are allowed by the selection rules for optical transitions in single-layer graphene [49].

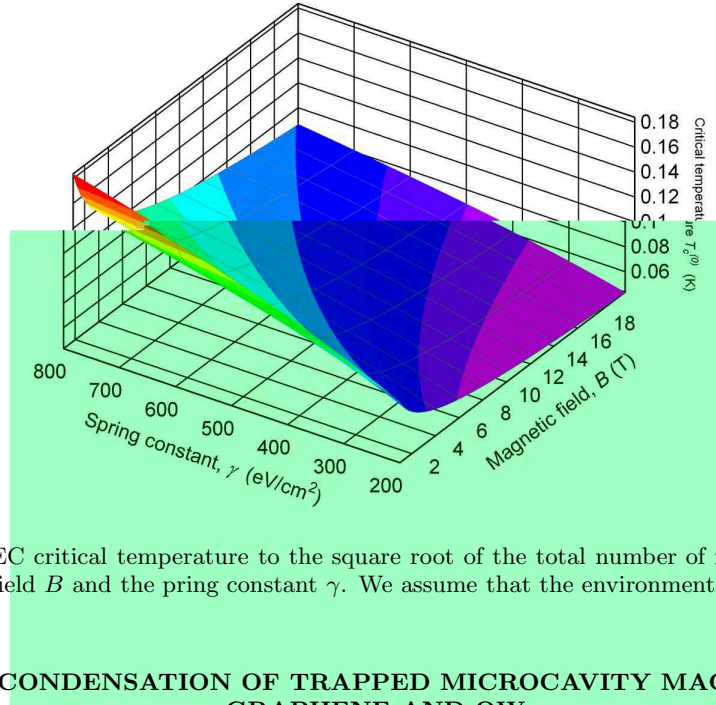


FIG. 4: The ratio of the BEC critical temperature to the square root of the total number of magnetopolaritons $T_c^{(0)}/\sqrt{N}$ as a function of the magnetic field B and the spring constant γ . We assume that the environment around graphene is GaAs with $\epsilon = 12.9$.

V. BOSE-EINSTEIN CONDENSATION OF TRAPPED MICROCAVITY MAGNETOPOLARITONS IN GRAPHENE AND QW

Although Bose-Einstein condensation cannot take place in a 2D homogeneous ideal gas at non-zero temperature, as discussed in Ref. [3], in a harmonic trap the BEC can occur in two dimensions below a critical temperature T_c^0 . Below we estimate this temperature. In a harmonic trap at a temperature T below a critical temperature T_c^0 ($T < T_c^0$), the number $N_0(T, B)$ of non-interacting magnetopolaritons in the condensate is given by [3]

$$\begin{aligned} N_0(T, B) &= N - \frac{\Gamma(2)\zeta(2) \left(g_s^{(e)} g_v^{(e)} + g_s^{(h)} g_v^{(h)} \right) M_{\text{eff}}(B)}{\hbar^2 \gamma_{\text{eff}}} (k_B T)^2 \\ &= N - \frac{\pi \left(g_s^{(e)} g_v^{(e)} + g_s^{(h)} g_v^{(h)} \right) M_{\text{eff}}(B)}{3\hbar^2 \gamma} (k_B T)^2, \end{aligned} \quad (57)$$

where N is the total number of magnetopolaritons, $g_s^{(e),(h)}$ and $g_v^{(e),(h)}$ are the spin and graphene valley degeneracies for an electron and a hole, respectively, k_B is the Boltzmann constant, $\Gamma(x)$ is the gamma function and $\zeta(x)$ is the Riemann zeta function.

Applying the condition $N_0 = 0$ to Eq. (57), and assuming that the magnetopolariton effective mass is given by Eq. (38), we obtain the BEC critical temperature $T_c^{(0)}$ for the ideal gas of magnetopolaritons in a single graphene layer in a magnetic field:

$$T_c^{(0)}(B) = \frac{1}{k_B} \left(\frac{3\hbar^2 \gamma N}{\pi \left(g_s^{(e)} g_v^{(e)} + g_s^{(h)} g_v^{(h)} \right) M_{\text{eff}}(B)} \right)^{1/2}. \quad (58)$$

At temperatures above $T_c^{(0)}$, the BEC of magnetopolaritons in a single graphene layer does not exist.

A three-dimensional plot of $T_c^{(0)}/\sqrt{N}$ as a function of magnetic field B and spring constant γ is presented in Fig. 4. In our calculations, we used $g_s^{(e)} = g_v^{(e)} = g_s^{(h)} = g_v^{(h)} = 2$. The functional relations between the spring constant γ and the magnetic field B corresponding to different constant values of $T_c^{(0)}/\sqrt{N}$ are presented in Fig. 5. According to Eq. (58), the BEC critical temperature $T_c^{(0)}$ decreases with the magnetic field as $B^{-1/4}$ and increases with the spring constant as $\gamma^{1/2}$. These functional relations are illustrated in Figs. 4, 5 and 6.

Substituting Eq. (58) into Eq. (57), we obtain

$$\frac{N_0(T, B)}{N} = 1 - \left(\frac{T}{T_c^{(0)}(B)} \right)^2. \quad (59)$$

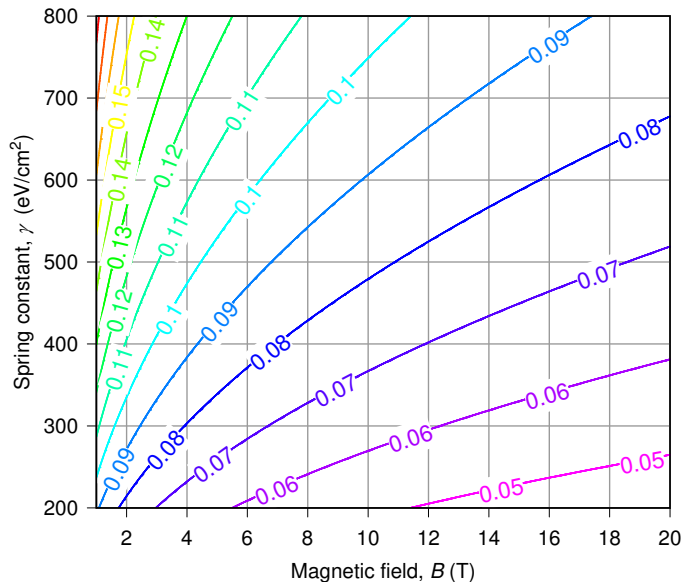


FIG. 5: The functional relations between the spring constant γ and the magnetic field B corresponding to the different constant values of $T_c^{(0)}/\sqrt{N}$. We assume that the environment around graphene is GaAs with $\epsilon = 12.9$.

Note that, since the quadratic spectrum of non-interacting magnetopolaritons given by Eq. (19) does not satisfy the Landau criterion of superfluidity [59, 60], the ideal Bose gas of magnetopolaritons in high magnetic field in graphene is not a superfluid.

Since magnetopolaritons in a QW are described by the same effective Hamiltonian as in graphene, but with the different magnetic mass of the magnetoexciton, the results of the calculations presented in Figs. 4, 5 and 6 for the critical temperature of the BEC for magnetopolaritons in graphene are valid for the BEC in a QW in a high magnetic field. This is true because the contribution to the effective mass of the magnetopolariton from the second term in the r.h.s. of Eq. (38) is much higher than from the first term.

VI. DISCUSSION AND CONCLUSIONS

In our calculations, we have assumed that the system under consideration is in thermal equilibrium. This assumption is valid if the relaxation time is less than the quasiparticle lifetime. Although the magnetopolariton lifetime is short, thermal equilibrium can be achieved within the regime of a strong pump. Porrás et al. [61] claimed that the time scale for polariton-exciton scattering can be small enough to satisfy this condition for the existence of a thermalized distribution of polaritons in the lowest k -states in a quantum well. We expect a similar characteristic time for magnetopolariton-magnetoexciton scattering in graphene. However, the consideration of pump and decay in a steady state may lead to results which are different from the ones presented in this paper. The consideration of the influence of decay on the BEC may be the subject of further studies of a trapped gas.

Above we discussed the BEC of the magnetopolaritons in a single graphene layer placed within a strong magnetic field. What would happen in a multilayer graphene system in a high magnetic field? Let us mention that the magnetopolaritons formed by the microcavity photons and the indirect excitons with the spatially separated electrons and holes in different parallel graphene layers embedded in a semiconductor microcavity can exist only at very low temperatures $k_B T \ll \hbar \Omega_R$. For the case of the spatially separated electrons and holes, the Rabi splitting Ω_R is very small in comparison to the case of electrons and holes placed in a single graphene layer. This is because $\Omega_R \sim d_{12}$ and the matrix element of magnetoexciton generation transition d_{12} is proportional to the overlapping integral of the electron and hole wavefunctions, which is very small if the electrons and holes are placed in different graphene layers. Therefore, we cannot predict the effect of relatively high BEC critical temperature for the electrons and holes placed in different graphene layers.

Spin polarization is important not only for the excitations but for the condensate itself. It was shown in [47, 48] that taking into account the spin degree of freedom can qualitatively modify the results for exciton-magnetopolariton condensation at magnetic fields lower than the critical magnetic field. We assume that magnetic field B under consideration is above the critical one and, therefore, the Zeeman splitting does not affect the spectrum of collective excitations according to Fig. 1 in [47]. So we neglect the Zeeman splitting in our calculations.

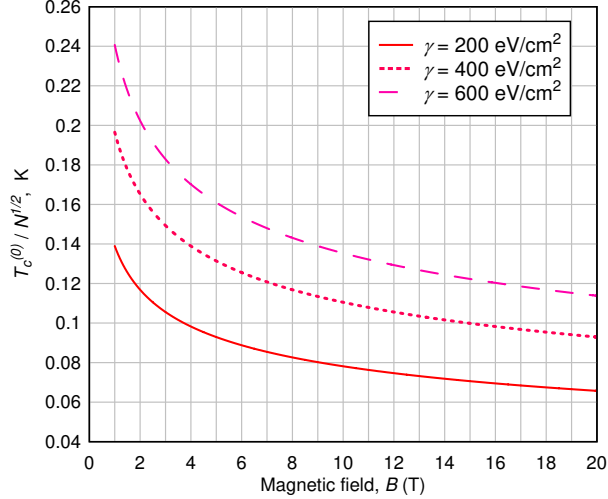


FIG. 6: The ratio of the BEC critical temperature to the square root of the total number of magnetopolaritons $T_c^{(0)}/\sqrt{N}$ as a function of magnetic field B at different spring constants γ . We assume the environment around graphene is GaAs with $\epsilon = 12.9$.

To conclude, we have derived the effective Hamiltonian of the ideal gas of trapped cavity magnetopolaritons in a single graphene layer and a QW in a high magnetic field. The resonance between magnetoexcitons and cavity photonic modes can be achieved either by controlling the spectrum of magnetoexcitons $\varepsilon_{ex}(P)$, by changing magnetic field B or by controlling the length of the microcavity L_C . We analyzed two possible physical realizations of the trapping potential: inhomogeneous local stress or a harmonic electric field potential coupled to magnetoexcitons and a parabolic shape of the semiconductor cavity causing the trapping of microcavity photons. We conclude that both realizations of confinement result in the same effective Hamiltonian. It is shown that the effective magnetopolariton mass M_{eff} increases with the magnetic field as $B^{1/2}$. Meanwhile, the BEC critical temperature $T_c^{(0)}$ decreases as $B^{-1/4}$ and increases with the spring constant as $\gamma^{1/2}$. The gas of magnetopolaritons in graphene and a QW in a high magnetic field can be treated as an ideal Bose gas since magnetoexciton-magnetoexciton interaction vanishes in the limit of a high magnetic field and a relatively high dielectric constant of the cavity $\epsilon \gg 2$, according to Sec. II. Let us mention that this condition for the high dielectric constant of the microcavity is valid only for graphene, and it is not valid for the quantum well. Observation of trapped cavity magnetopolaritons in graphene in a high magnetic field would be an interesting confirmation of the magnetopolaritonic BEC that we have described. Besides, we have obtained the Rabi splitting related to the creation of a magnetoexciton in a high magnetic field in graphene. Since this Rabi splitting is proportional to $B^{-1/4}$, we conclude that the Rabi splitting in graphene can be controlled by the external magnetic field B , while in a quantum well the Rabi splitting does not depend on the magnetic field when it is strong. The results for the critical BEC temperature of magnetopolaritons in a QW and graphene in high magnetic field are similar, since the magnetoexcitons in both systems are described by the same Hamiltonian.

Acknowledgments

We would like to thank J. F. Vazquez-Poritz for the useful discussion. O. L. B., R. Ya. K. were supported by PSC CUNY grant 621360040, and Yu. E. L. was partially supported by INTAS and RFBR grants.

-
- [1] *Physica Status Solidi B* **242**, 1 (2005), special issue of Physics of Semiconductor Microcavities, edited by B. Deveaud.
- [2] A. Kavokin and G. Malpeuch, *Cavity Polaritons* (Elsevier, 2003).
- [3] V. Bagnato and D. Kleppner, *Phys. Rev. A* **44**, 7439 (1991).
- [4] P. Nozières, in *Bose-Einstein Condensation*, A. Griffin, D. W. Snoke, and S. Stringari, Eds. (Cambridge Univ. Press, Cambridge, 1995), p.p. 15-30.
- [5] R. Balili, D. W. Snoke, L. Pfeiffer, and K. West, *Appl. Phys. Lett.* **88**, 031110 (2006).
- [6] R. Balili, V. Hartwell, D. W. Snoke, L. Pfeiffer and K. West, *Science* **316**, 1007 (2007).
- [7] O. L. Berman, Yu. E. Lozovik, and D. W. Snoke, *Phys. Rev. B* **77**, 155317 (2008).
- [8] J. Kasprzak, et. al., *Nature* **443**, 409 (2006).
- [9] T. Ando, A. B. Fowler, and F. Stern, *Rev. Mod. Phys.* **54**, 437 (1982).
- [10] K. S. Novoselov, A. K. Geim, S. V. Morozov, D. Jiang, Y. Zhang, S. V. Dubonos, I. V. Grigorieva, and A. A. Firsov, *Science* **306**, 666 (2004).
- [11] Y. Zhang, J. P. Small, M. E. S. Amori, and P. Kim, *Phys. Rev. Lett.* **94**, 176803 (2005).
- [12] K. S. Novoselov, A. K. Geim, S. V. Morozov, D. Jiang, M. I. Katsnelson, I. V. Grigorieva, and S. V. Dubonos, *Nature (London)* **438**, 197 (2005).
- [13] Y. Zhang, Y. Tan, H. L. Stormer, and P. Kim, *Nature (London)* **438**, 201 (2005).
- [14] K. Kechedzhi, O. Kashuba, and V. I. Fal'ko, *Phys. Rev. B* **77**, 193403 (2008).
- [15] M. I. Katsnelson, *Europhys. Lett.* **84**, 37001 (2008).
- [16] A. H. Castro Neto, F. Guinea, N. M. R. Peres, K. S. Novoselov, and A. K. Geim, *Rev. Mod. Phys.* **81**, 109 (2009).
- [17] S. Das Sarma, E. H. Hwang, and W.-K. Tse, *Phys. Rev. B* **75**, 121406(R) (2007).
- [18] K. Nomura and A. H. MacDonald, *Phys. Rev. Lett.* **96**, 256602 (2006).
- [19] C. Töke, P. E. Lammert, V. H. Crespi, and J. K. Jain, *Phys. Rev. B* **74**, 235417 (2006).
- [20] V. P. Gusynin and S. G. Sharapov, *Phys. Rev. B* **71**, 125124 (2005).
- [21] V. P. Gusynin and S. G. Sharapov, *Phys. Rev. Lett.* **95**, 146801 (2005).
- [22] O. Vafek, *Phys. Rev. Lett.* **97**, 266406 (2006).
- [23] A. Iyengar, J. Wang, H. A. Fertig, and L. Brey, *Phys. Rev. B* **75**, 125430 (2007).
- [24] Z. G. Koinov, *Phys. Rev. B* **79**, 073409 (2009).
- [25] D. W. Snoke, *Science* **298**, 1368 (2002).
- [26] L. V. Butov, *J. Phys.: Condens. Matter* **16**, R1577 (2004).
- [27] V. B. Timofeev and A. V. Gorbunov, *J. Appl. Phys.* **101**, 081708 (2007).
- [28] J. P. Eisenstein and A. H. MacDonald, *Nature* **432**, 691 (2004).
- [29] Yu. E. Lozovik and V. I. Yudson, *JETP Lett.* **22**, 26(1975); *JETP* **44**, 389 (1976); *Physica A* **93**, 493 (1978).
- [30] X. Zhu, P. Littlewood, M. Hybertsen and T. Rice, *Phys. Rev. Lett.* **74**, 1633 (1995).
- [31] G. Vignale and A. H. MacDonald, *Phys. Rev. Lett.* **76** 2786 (1996).
- [32] Yu. E. Lozovik and O. L. Berman, *JETP Lett.* **64**, 573 (1996); *JETP* **84**, 1027 (1997).
- [33] I. V. Lerner and Yu. E. Lozovik, *JETP* **51**, 588 (1980); *JETP*, **53**, 763 (1981); A. B. Dzyubenko and Yu. E. Lozovik, *J. Phys. A* **24**, 415 (1991).
- [34] D. Paquet, T. M. Rice, and K. Ueda, *Phys. Rev. B* **32**, 5208 (1985).
- [35] C. Kallin and B. I. Halperin, *Phys. Rev. B* **30**, 5655 (1984); *Phys. Rev. B* **31**, 3635 (1985).
- [36] D. Yoshioka and A. H. MacDonald, *J. Phys. Soc. Japan* **59**, 4211 (1990).
- [37] Yu. E. Lozovik and A. M. Ruvinsky, *Phys. Lett. A* **227**, 271 (1997); *JETP* **85**, 979 (1997).
- [38] M. A. Olivares-Robles and S. E. Ulloa, *Phys. Rev. B* **64**, 115302 (2001).
- [39] S. A. Moskalenko, M. A. Liberman, D. W. Snoke and V. V. Botan, *Phys. Rev. B* **66**, 245316 (2002).
- [40] O. L. Berman, Yu. E. Lozovik, and G. Gumbs, *Phys. Rev. B* **77**, 155433 (2008).
- [41] O. L. Berman, R. Ya. Kezerashvili, and Yu. E. Lozovik, *Phys. Rev. B* **78**, 035135 (2008).
- [42] O. L. Berman, R. Ya. Kezerashvili, and Yu. E. Lozovik, *Phys. Lett. A* **372** 6536 (2008).
- [43] Yu. E. Lozovik and A. A. Sokolik, *JETP Lett.* **87**, 55 (2008); Yu. E. Lozovik, S. P. Merkulova, and A. A. Sokolik, *Physics-Uspokhi*, **51**, 727 (2008) (translated from *Usp. Fiz. Nauk* **178**, 757 (2008), in Russian).
- [44] H. Min, R. Bistritzer, J.-J. Su, and A. H. MacDonald, *Phys. Rev. B* **78**, 121401(R) (2008).
- [45] R. Bistritzer and A. H. MacDonald, *Phys. Rev. Lett.* **101**, 256406 (2008).
- [46] M. Yu. Kharitonov and K. B. Efetov, *Phys. Rev. B* **78**, 241401(R) (2008).
- [47] Yu. G. Rubo, A. V. Kavokin, and I. A. Shelykh, *Phys. Lett. A* **358**, 227 (2006).
- [48] T. C. H. Liew, Yu. G. Rubo, I. A. Shelykh, and A. V. Kavokin, *Phys. Rev. B* **77**, 125339 (2008).
- [49] V. P. Gusynin, S. G. Sharapov, and J. P. Carbotte, *J. Phys.: Condens. Matter* **19**, 026222 (2007).
- [50] Yu. E. Lozovik and A. M. Ruvinskii, *JETP* **87**, 788 (1998).

- [51] V. Lukose, R. Shankar, and G. Baskaran, *Phys. Rev. Lett.* **98**, 116802 (2007).
- [52] L. P. Gorkov and I. E. Dzyaloshinskii, *Sov. Phys. JETP* **26**, 449 (1967).
- [53] S. Pau, G. Björk, J. Jacobson, H. Cao and Y. Yamamoto, *Phys. Rev. B* **51**, 14437 (1995).
- [54] C. Ciuti, P. Schwendimann, and A. Quattropani, *Semicond. Sci. Technol.* **18**, S279 (2003).
- [55] L. Pitaevskii and S. Stringari, *Bose-Einstein Condensation*, Clarendon Press, Oxford (2003).
- [56] J. P. Fernández and W. J. Mullin, *J. Low. Temp. Phys.* **128**, 233 (2002).
- [57] O. L. Berman, Yu. E. Lozovik, D. W. Snoke, and R. D. Coalson, *Phys. Rev. B* **73**, 235352 (2006).
- [58] Y. Zheng and T. Ando, *Phys. Rev. B* **65**, 245420 (2002).
- [59] A. A. Abrikosov, L. P. Gorkov and I. E. Dzyaloshinski, *Methods of Quantum Field Theory in Statistical Physics* (Prentice-Hall, Englewood Cliffs. N.J., 1963).
- [60] A. Griffin, *Excitations in a Bose-Condensed Liquid* (Cambridge University Press, Cambridge, England, 1993).
- [61] D. Porras, C. Ciuti, J. J. Baumberg, and C. Tejedor, *Phys. Rev. B* **66**, 085304 (2002).